

# About the Lorentz Correction Used in the Interpretation of Small Angle X-Ray Scattering Data of Semicrystalline Polymers

F. CSER\*

Cooperative Research Centre for Polymers, 32 Business Drive, Notting Hill, VIC 3168, Australia

Received 20 December 1999; accepted 5 May 2000

**ABSTRACT:** Lorentz correction is used to correct the intensities of X-ray scattering of single crystal diffractometry in order to recalculate intensities to obtain structure factors. This correction reduces the intensities to zero at zero diffraction angle. Small angle scattering is used to study the dimensions of heterogeneities in polymeric materials. The scattering intensities near to zero scattering angle originate partly from periodic systems (reciprocal lattice) and partly from dispersed particle systems. Periodic systems should result in individual Gaussian or Lorentzian peaks with the position of a peak maximum depending on the length of the periodicity. Particle scattering results in a Gaussian peak centred at zero scattering angle. The effect of the Lorentz correction on the interpretation of small angle X-ray scattering data is shown in the case of some semicrystalline polyethylenes (high density, linear low density, and low molecular weight waxy polyethylenes). The data are compared with those for amorphous block copolymers (styrene/butadiene) in which there is a periodic system with homogeneous lamellar thickness. Lorentz correction destroys the characteristics of the particle scattering and can be applied only for periodic systems. It should not be used to produce a peak on scattering data which does not show periodicity (peaks) without correction. © 2001 John Wiley & Sons, Inc. *J Appl Polym Sci* 80: 2300–2308, 2001

**Key words:** small angle X-ray scattering; diffraction; semicrystalline polymers; polyethylene; Lorentz correction

## INTRODUCTION

The structures of semicrystalline polymers, including polyethylenes of different types, are supposed to consist of periodically arranged crystalline lamellae, which are separated by amorphous phases. The layer thicknesses of the crystalline and amorphous layers are fairly homogeneous.<sup>1,2</sup> The length of the periodicity ( $d$ ) is calculated from

the position of the peak maximum in the X-ray intensities using the Bragg equation :

$$d = \frac{\lambda}{2 \sin(\Theta)} \quad (1)$$

where  $\Theta$  is half of the diffraction angle of the peak maximum and  $\lambda$  is the wavelength of the X-ray.

This formula is applied to calculate the length of periodic systems, i.e., systems that can be described by a reciprocal lattice. The lamellar thickness of the crystals is generally calculated from the Bragg periodicity and modified by the percent crystallinity of the system determined either from

\* Present address: Polymer Technology Centre, RMIT University, Melbourne, VIC 3000, Australia (ferenc.cser@rmit.edu.au).

*Journal of Applied Polymer Science*, Vol. 80, 2300–2308 (2001)  
© 2001 John Wiley & Sons, Inc.

wide angle X-ray diffraction (WAXS), from differential scanning calorimetry (DSC) heat flow data or from density measurements (see, e.g., Ref.<sup>3</sup>).

Small angle X-ray scattering (SAXS) is also used to determine particle size and its distribution in such systems where the particles (or a second phase in a broader sense) are dispersed in a continuous phase called the matrix.<sup>4,5</sup> This is the case of so-called particle scattering.

The conditions to use SAXS for these kinds of systems are the following: (a) the electron densities of the particle and the matrix must be different; (b) the electron density of the matrix must be constant at larger distances from the particles; (c) the structure must be statistically isotropic; and (d) there should be no long range order, so that there is no correlation between two points separated widely enough. These conditions are generally fulfilled in a diluted solution of macromolecules but generally not in the semicrystalline polymeric bulk. There is a 10–15% difference in the electron densities of the amorphous and the crystalline phase, so condition (a) is generally fulfilled. As the crystallinity varies from 10 to 60%, in most of the systems used for the study, conditions (b) and (d) are not fulfilled: the dimension and the volume of the amorphous phase are commensurable to those of the crystalline one. If the crystals form folded chain lamellae with a fairly homogeneous thickness,<sup>1</sup> condition (c) is also not fulfilled as lamellae with extended lateral dimension with respect to their thickness cannot be packed isotropically. There must be a local order of the lamellar particles as well as the amorphous environment around the particles.

The scattering intensities of a particle system is the Fourier transform of the electron densities that reduces for the conditions shown above to the form described by eq. (2):

$$I(\mathbf{s}) = \int 4\pi\mathbf{r}^2 d\mathbf{r}\bar{\rho}^2(\mathbf{r}) \frac{\sin(\mathbf{s}\mathbf{r})}{\mathbf{s}\mathbf{r}} \quad (2)$$

where  $\mathbf{r}$  represents the position vector in the real space, and  $\mathbf{s}$  represents that of the reciprocal space. This latter term is expressed by eq. (3):

$$\mathbf{s} = \frac{4\pi}{\lambda} \sin(\Theta) \quad (3)$$

The solution of eq. (2) in the case of spheres with radius of  $\mathbf{r}$  is given by eq. (4)<sup>6</sup>:

$$I(\mathbf{s}) = V^*(\rho_p - \rho_m)^2 * 3 * \left( \frac{\sin(\mathbf{s}\mathbf{r}) - \mathbf{s}\mathbf{r} * \cos(\mathbf{s}\mathbf{r})}{(\mathbf{s}\mathbf{r})^3} \right)^2 \quad (4)$$

where  $\rho_p$  and  $\rho_m$  are the electron densities of the particle and of the matrix respectively, and  $V$  is the volume of the particles. This function forms approximately a Gaussian peak centred at  $\mathbf{s} = 0$ .

Guinier<sup>6</sup> presented an approximation to describe the scattering intensity near to zero scattering angle using the radius of gyration of the particle system shown by eq. (5):

$$I = I_0 \exp(-KR^2\Theta^2) \quad (5)$$

where  $I_0$  represents the scattering intensity at zero angle,  $R$  is the radius of gyration of the particle and  $\Theta$  is half of the scattering angle.  $K$  is a universal constant ( $16\pi^2/3\lambda^2$ ).

Equations (2), (4), and (5) show that X-ray scattering of particles has a maximum at zero angle with an approximately Gaussian shape of the scattering toward greater angles. This means X-ray scattering for particles has nonzero values at zero diffraction angle. The  $\log(I)$  versus square of the scattering vector  $\mathbf{s}$  (the Guinier plot) results in a straight line with a slope corresponding to the Gaussian scattering curve and this slope can be used to determine the dimension (radius of gyration) of the scattering particle.

There is another relationship used in SAXS data processing, the so-called invariant ( $Q$ ),<sup>5</sup> that is expressed by eq. (6):

$$Q = \int_{\mathbf{r}=0}^{\infty} I(\mathbf{s})\mathbf{s}^2 d\mathbf{s} \quad (6)$$

The invariant is expressed as an integral of the intensities multiplied by the square of the scattering vector. The importance of the invariant is that it expresses a factor by which the structural data can be reduced to an absolute scale without having to measure the absolute intensities. The invariant represents the scattering power of the particles with respect to the matrix and their concentration as it is expressed by eq. (7):

$$Q \approx (\rho_p - \rho_m)^2 * \Phi_p * (1 - \Phi_p) \quad (7)$$

where  $\rho_p$  and  $\rho_m$  are the electron densities for the particles and for the matrix, respectively, and  $\Phi_p$  is the volume fraction of the particles. Equation

(7) states that the integral of the corrected intensities is proportional to the square of the difference in the electron densities of the matrix and that of the particles as well as to their volume. In the case of semicrystalline polymers, this function has a maximum at 50% of crystallinity. The invariant was calculated and used for representing the actual crystallinity of the polymer as a function of the temperature in a number of investigations.<sup>7-9</sup>

Another approach of a real polymeric structure is a fractal type.<sup>10</sup> In this case, the intensity function is reciprocal proportional to the  $t$ -th power of the scattering vector  $\mathbf{s}$  as it is expressed by eq. (8):

$$I(\mathbf{s}) = I(0) * \mathbf{s}^{-t} \quad (8)$$

where  $t$  is the fractal coefficient. The intensity at zero angle has a finite value in this case, also.

## THE LORENTZ CORRECTION

The Lorentz correction means a multiplication of the scattering intensities by a factor proportional to the sine of the diffraction angle. This correction is generally used in single crystal X-ray crystallography to correct the X-ray intensities obtained from crystalline materials to calculate correct structure factor values independent on the geometry of data collection [see, e.g., eq. (2) in Ref.<sup>11</sup>]. It corrects the differences in the time that the individual reciprocal lattice point, with different indices and consequently being at different distance from the origin ([000]), spends on the surface of the Ewald sphere, i.e., it is in diffracting position. It is applied only to scattering from the reciprocal lattices where there is a periodicity with a great number of consecutive cells in the crystalline systems. This correction eliminates the intensity at zero angle, as [000] is always in a diffracting position. The factor contains a  $\sin(2\theta)$  element and other elements that are dependent on the geometry of the data collection, i.e., intensity measurement.

Recently, much of the work dealing with SAXS of semicrystalline materials uses a so-called Lorentz correction<sup>3,7-9,12-16</sup> in trying to determine the periodicity of the structure. The authors do not use a multiplication factor of  $\sin(2\theta)$ ; they generally use its squared form. In most of these cases this correction is used, even when there is not any peak on the uncorrected SAXS intensity

curve. This means that there is no indication that a reciprocal lattice would be present in the system. Some other authors do not use this correction.<sup>10,17,18</sup>

As seen above, in the case of particle scattering, the maximum of the scattering intensities is at zero scattering angles. If Lorentz correction is applied, the nearly Gaussian shape of the scattering intensities is destroyed, reducing the intensities to zero at zero diffraction angle, and an artificial maximum might be produced on the curve. The position of this maximum depends on the dimension and the volume of the phases as well as on the difference in the electron density of the particles and the matrix.

The scattering curve of a real system is always the sum of the scattering intensities of the different phases and interactions between the phases. In a periodic lamellar system, a reciprocal axis is present and therefore produces a peak (or series of peaks) in the scattering curves and their exact position might be determined from the Lorentz-corrected intensities. If there are also particles or fractals in the system, their characteristic scattering will be superposed on the scattering caused by the reciprocal lattice and a Lorentz correction will destroy the shape of the curve. In this case, it cannot be used for structural calculations. The sum of the intensities originating from the particle scattering might shift the position of the peaks derived from the reciprocal lattice and their position will also be incorrect. Therefore, the two scattering types must be separated from each other and handled individually as Dlugosz et al.<sup>12</sup> suggested in their article where Lorentz correction was introduced and used for obtaining the exact peak position of a Bragg peak near to the zero diffraction angle.

Polyethylene (PE) has been the subject of SAXS investigations since its existence. PE has a broad maximum in the SAXS intensities.<sup>1,8,16,19,20</sup> This maximum is claimed to represent the repeating period of the lamellar structure of the crystallites.<sup>1</sup> In some previous and only partially published<sup>21</sup> work on SAXS of semicrystalline polymers, the SAXS curves of many PEs [high density (HDPE), linear low density (LLDPE), or low density (LDPE)] as well as polypropylenes (PPs) and their blends did not show definite maxima to indicate the dominance, or even the presence, of a reciprocal lattice type of structure. Therefore, the Lorentz correction was abandoned and the system was handled as particles dispersed in a matrix or as a fractal. In this report, SAXS intensi-

ties of some PEs are presented as examples to show the effect of the Lorentz correction on the structural data derived from the original experiments. The same data are shown in two different interpretations, e.g., as a reciprocal lattice and as dispersed particles, to be able to discuss the effect of the Lorentz correction on the possible interpretation of the data. The hypothetical models of polymeric crystals are disregarded for the interest of the study. WAXS data are also shown to give a proper characterization of the semicrystalline polymeric systems. SAXS data on block copolymers with polystyrene and polybutadiene blocks of narrow molecular weight distribution are also shown as a comparison.

## EXPERIMENTAL

### Materials

The materials included the following: HDPE: extrusion grade polymer, MFI: 1 g/min; C6-LLDPE: gas phase polymerized LLDPE with hexene comonomer,  $\rho = 922 \text{ kg/m}^3$ , MFI: 0.78 g/10 min; PE-wax: oligo-ethylene, extracted from LLDPE,  $M_w \sim 1000 \text{ g/mol}$ ,  $\rho = 980 \text{ kg/m}^3$ ; SEBS: poly(styrene-*block*-ethylene-*co*-butadiene),  $M_w = 43,000$ , styrene content: 25%; and SBS: poly(styrene-*block*-butadiene),  $M_w = 39,000$ , styrene content: 25%.

### Sample Preparation

Compression-molded sheets of HDPE, SBS, SEBS, and PE-wax with a thickness of 2–3 mm were used for this study. From C6-LLDPE, a stack of blown films with an individual thickness of 0.025 mm and an overall thickness of 2 mm was studied. SAXS and WAXS intensities were recorded in the machine direction (MD) and the transverse direction (TD) using the axes of the blown cylinder as the MD.

### X-Ray Diffractometry

A Rigaku Geigerflex generator was used with a wide angle and a Kratky type small angle goniometer. A 30-kV accelerating voltage and a 30-mA current was applied using Ni-filtered Cu-K $\alpha$  radiation.

WAXS intensities were collected from  $2\Theta = 3$  to  $50^\circ$  with steps of  $0.05^\circ$  using transmission techniques on the compression-molded or multiple-

layered film samples. Data were collected and processed using separate graphic software.

SAXS intensities were collected from  $2\Theta = -1$  to  $1^\circ$  in steps of  $0.002^\circ$  using the same samples as for WAXS. Background intensities were collected for each type of sample (thickness, absorption) from the same sample positioned just in front of the counter. Data were collected and processed using a computer program for removing the background and calculating the average of the data from the two sides of the primary beam. Slit correction (desmearing) was applied. For this purposes, the derivative of the intensity data were obtained by a smooth derivation using two neighboring data points at each side. A numerical integration was performed on smoothed derivatives using limits of the data collection ( $\mathbf{s}_0$ ,  $\mathbf{s}_e$ ) for the integration according eq. (9):

$$I(\mathbf{s}) = -\frac{1}{\pi} \int_{\mathbf{s}_0}^{\mathbf{s}_e} \frac{I(\sqrt{\mathbf{s}^2 + t^2})}{\sqrt{\mathbf{s}^2 + t^2}} dt \quad (9)$$

The maximum resolution of the SAXS camera was 120 nm as the intensities could generally be collected up to  $2\Theta = 0.06^\circ$ . SAXS intensities from PE-wax were collected from  $0.06$  to  $5^\circ$  in  $2\Theta$ . These data were not corrected for the background.

Melting enthalpies were determined by temperature-modulated DSC (TMDSC) integrating the total heat flow from  $0^\circ\text{C}$  to the end of the melting peaks. A heating rate of 2 K/min was used with 40 s as modulation period and 0.6 K as modulation amplitude in a TA Instrument TMDSC equipped with an intercooler device. Helium flushing gas with a 25-mL/min flow rate was used.

## RESULTS AND DISCUSSION

Figures 1–3 show the WAXS intensities of the PE sample materials. HDPE and PE-wax show normal orthorhombic crystalline modification of PE.<sup>17,18</sup>

The amorphous scattering intensities were removed from the scattering intensities and the intensities of the pure crystalline phases are also shown in Figures 1 and 2. There is a broad maximum with a peak position at  $2\Theta = 13^\circ$ . This maximum is always present and its intensity is proportional to the amount of the crystalline phase, i.e., it cannot be included in the scattering

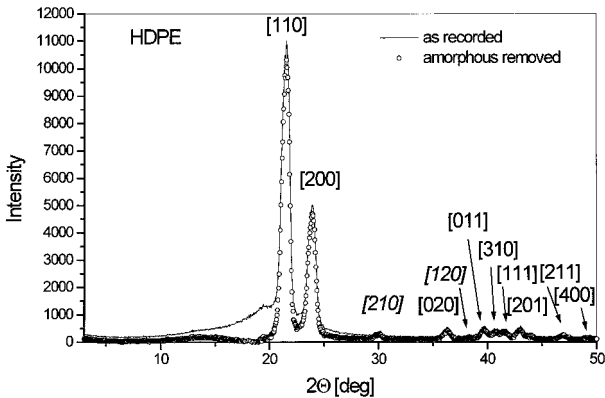


**Figure 1** WAXS intensities of HDPE. Total and crystalline diffraction.

intensities of the amorphous phase. Liquid polyisobutylene has a broad amorphous diffraction peak at this scattering angle. The crystallinity of the HDPE is 75%, and the crystallinity for PE-wax and C6-LLDPE is 67% and 53%, respectively (TMDSC result).

There are two peaks in the WAXS intensities of PE-wax corresponding to a lamellar period as shown in Figure 2. The maxima of the peaks are at 3.3 and 5.1°, respectively. The  $l$  indices of the lamellar phase are underlined; those without underlining indicate the  $l$  indices of the PE sub-cell ( $c = 2.53 \text{ \AA}$ ).

The film blown from C6-LLDPE shows a strong orientation effect. There is an  $a$ - $b$  orientation in the plane of the film. The diffraction peak with the index of [200] is high in the MD and low in the TD. The [020] peak is absent in the MD and

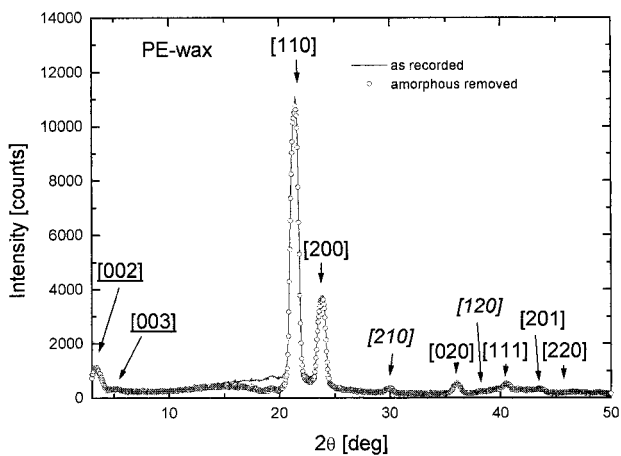


**Figure 2** WAXS intensities of a high molecular weight wax. Total and crystalline diffraction.

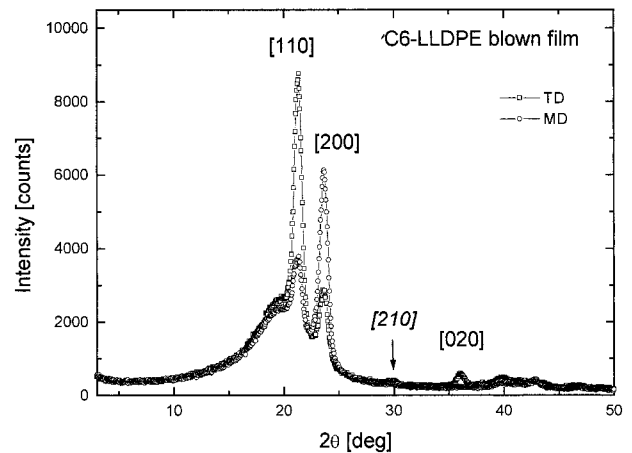
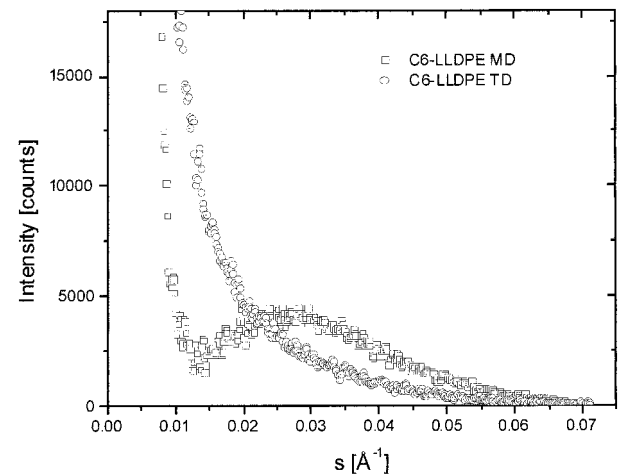


**Figure 3** WAXS intensities of C6-LLDPE blown films recorded in two orthogonal directions.

present in the TD. The [110] peak is low in the MD as well.

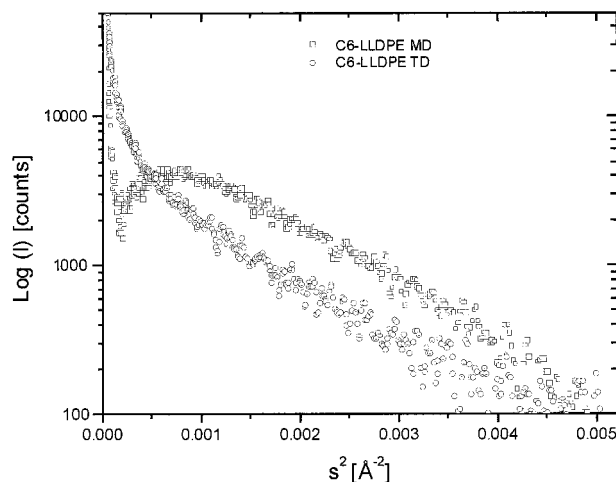
SAXS intensities of C6-LLDPE systems are shown in Figure 4. The intensities recorded in the TD and in the MD are different. There is no indication of a peak in the TD but a very broad peak can be seen in the MD. The corresponding Bragg periodicity is 23 nm. The crystallinity of C6-LLDPE is calculated as 44.8% from the melting enthalpy (130 J/g) and 55% on the basis of the density using  $850 \text{ kg} \cdot \text{m}^{-3}$  for the amorphous and  $1005 \text{ kg} \cdot \text{m}^{-3}$  for the crystalline PE, respectively.<sup>10</sup> The lamellar thickness of the crystallites is estimated to be  $\sim 10 \text{ nm}$ .

Figure 5 shows the Guinier representation of the same intensities shown in Figure 4. The curve



**Figure 4** Desmeared SAXS intensities of C6-LLDPE film recorded in two orthogonal (machine and transverse) directions.





**Figure 5** Desmeared SAXS intensities of C6-LLDPE. Guinier representation of the data shown in Figure 4.

recorded in the TD can be represented by the combination of two straight lines, which relate to particle scattering in the TD. The radii of gyration determined from the initial slope in the TD is 17 nm and that for the second part is 5.2 nm. The corresponding lamellar thicknesses are 59 and 21 nm. These values show much greater lamellar thickness than those estimated from the Bragg period. There is a broad peak superimposed on the straight lines representing a combined particle scattering in the MD.

Figure 6 shows the Lorentz-corrected intensities of the same system. Both curves show a maximum. The maxima correspond to 25 nm in the

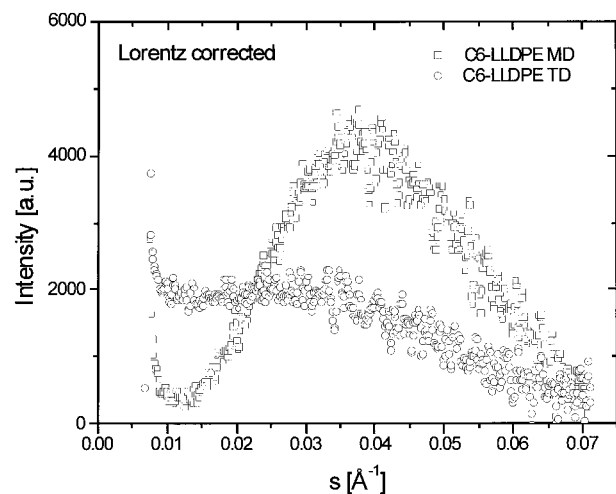


**Figure 6** Lorentz-corrected SAXS intensities of C6-LLDPE derived from the data shown in Figure 4.

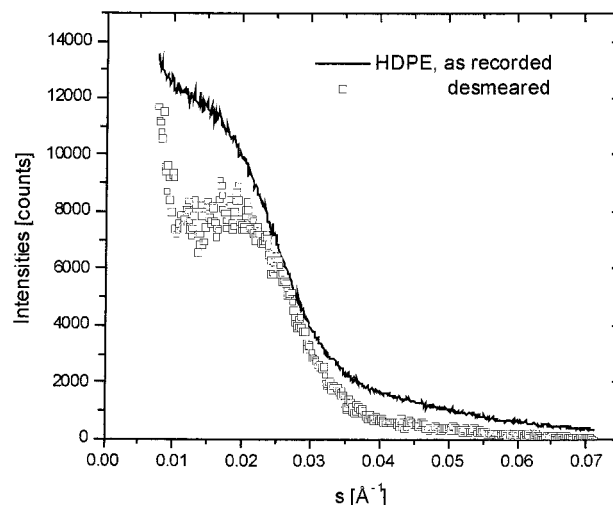


**Figure 7** As-recorded and desmeared SAXS intensities of HDPE.

TD and 16 nm in the MD, which leads to the lamellar thickness of the crystallites of 7–11 nm.

The measured peak melting temperature of C6-LLDPE is 125.3°C, which corresponds to a lamellar thickness of 16 nm using the Thomson-Gibbs formula<sup>12</sup>:

$$T_m = T_m^0 * \left( 1 - \frac{2\sigma_c}{\Delta H_u * L_c} \right) \quad (10)$$

where  $T_m$  is the melting temperature of a crystal with a thickness of  $L_c$  (cm).  $T_m^0$  is the extrapolated melting temperature of the crystals with infinite thickness (414 K),  $\sigma_c$  is the surface free energy ( $8.7 \mu\text{J} \cdot \text{cm}^{-2}$ ) and  $\Delta H_u$  is the molar heat of fusion ( $2.9 \cdot 10^2 \text{ J} \cdot \text{cm}^{-3}$ ). The reference data in brackets is for polymethylene and comes from Ref.<sup>12</sup>

The Lorentz-corrected scattering curves resulted in much smaller lamellar thickness for the crystallites than estimated from the melting peak temperatures. The particle size obtained from the Guinier approximation is much closer to the value expected from the melting peak temperature.

Figure 7 shows the as-recorded and the desmeared SAXS intensities of HDPE. There is a peak at  $s = 0.026 \text{ \AA}^{-1}$  corresponding to a lattice parameter of 25 nm. The melting enthalpy of HDPE is 205 J/g, which corresponds to 70.6% of crystallinity. The lamellar thickness of the crystallites is 17 nm. Figure 8 shows the Lorentz-corrected intensities of HDPE. There are two peaks in the curve that correspond to 26- and 13-nm Bragg periods. The melting temperature of

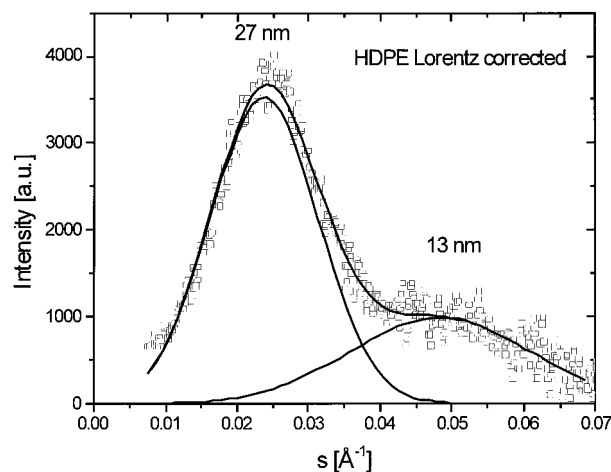


**Figure 8** Lorentz-corrected SAXS intensities of HDPE. Evolution of two Bragg peaks.

this HDPE was 131°C as observed from the TMDSC endotherm. Using the actual peak melting temperature and eq. (10), the calculated lamellar thickness is 36 nm. The Bragg periods read from the peak positions are much smaller than the value expected on the basis of the melting peak temperature.

The two peaks have half line widths of 0.0021 and 0.0036 rad. This corresponds to  $N_c = 2.9$  and 3.5 cells within a crystalline “particle” according to the Scherer formula :

$$B = \frac{K * \lambda}{N_c * d * \cos(\Theta_0)} \quad (11)$$

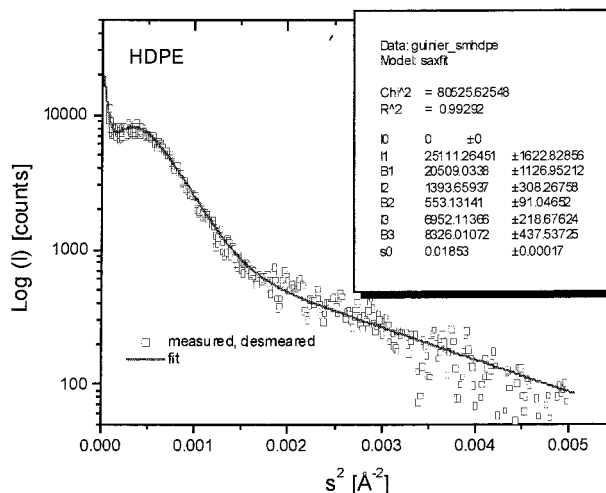
where  $N_c$  is the number of crystalline units with periodical length of  $d$ ,  $B$  is the half width of the diffraction peak expressed in rad, and  $K$  is a constant with a value of 1.07.  $N_c$  numbers are very small. This means that the peaks cannot be diffraction peaks as a result of a true reciprocal lattice. These numbers reflect a liquid structure rather than a crystalline one. The same conclusion can be drawn for C6-LLDPE, where the line widths (0.0051 and 0.0063 rads) yielded 2.4 and 1 for the number in unit cells of the particle in the two directions, respectively.

The desmeared data are now handled as a superposition of the particle and crystalline scattering as suggested by Dlugosz et al.<sup>12</sup> A least square fit was calculated using two different kinds of particles and a reciprocal lattice according to eq. (12):

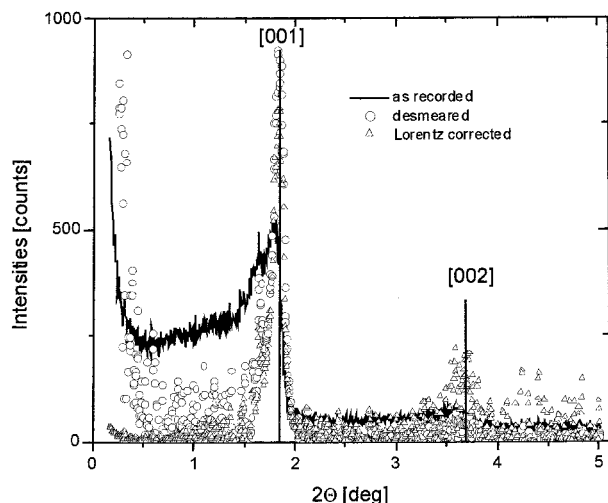
$$I = I_1^0 * \exp(-B_1 * s^2) + I_2^0 * \exp(-B_2 * s^2) + I_3^0 * \exp(-B_3 * (s_0^3 - s)^2) \quad (12)$$

Figure 9 shows the fit and the refined parameters. The fit is excellent. If the areas under the individual peaks are considered, the reciprocal lattice type diffraction has less than 10% weight of the total scattering intensities. The line width of the Gauss peak for a reciprocal lattice scattering was 0.0016 rad, what is another unrealistic value. The maximum corresponds to a periodicity of 57 nm. This results in a number of unit cells equal to 1.8 using the Scherer formula. The Lorentz correction had a smaller effect to the calculated periodicities when there had been a peak in the scattering intensities.

SAXS studies on PE-wax served to prove that the equipment is suitable to produce proper SAXS data as well as to show the upper limit of line broadening due to the equipment (instrumental line broadening). Figure 10 shows the SAXS intensities of the PE-wax as recorded together with the desmeared as well as the Lorentz-corrected values of the latter one. As expected, [001] is present together with [002], which was indicated in Figure 2 (at  $2\Theta = 3.3^\circ$ ), and the peaks are asymmetric in the as recorded data, because of the smearing of the line slit. The Lorentz-correction brought [002] in a commensurable intensity with [001]; nevertheless, the position of the maximum did not change. The maxima correspond to a 4.85-nm periodicity. The particle size of the crystals along the  $c$  axis is 72 or 47 nm estimated from the line broadening without the correction of the instrumental broadening (0.0023 and 0.0030 rad). This means that there are at least 15–19



**Figure 9** Desmeared SAXS intensities of HDPE. The fit of the two phase model (reciprocal lattice and particle scattering).



**Figure 10** Comparison of the as-recorded, desmeared, and Lorentz-corrected SAXS intensities of high molecular weight wax.

consecutive unit cells in this direction. This is in the range of relatively small crystals. Using proper instrumental line broadening, this number is higher. There is negligible scattering intensity caused by particle scattering despite the presence of a measurable amorphous phase. The melting enthalpy of the PE-wax is 194 J/g, which corresponds to 67% of crystallinity. The WAXS curves suggested a much greater value (95%). The melting temperature of the PE-wax is 60°C. This corresponds to a lamellar thickness of 3.1 nm. Using the measure of crystal particle size determined without the Lorentz correction (i.e., 45 nm) and the TMDSCX crystallinity, the crystalline lamellar thickness is calculated to be 3.3 nm. This fits quite well the value estimated by the Thomson-Gibbs formula.

As a comparison again, Figure 11 shows the SAXS intensities of two block copolymers of styrene and butadiene in a Guinier representation. One of the copolymers has been partially hydrogenated. There are peaks on the scattering intensity curves corresponding to 27–29-nm periodicity. When the desmeared intensities are compared with those of the Lorentz-corrected ones (see Fig. 12), only a small shift in the peak position can be detected in the direction of the smaller periodicities (26 nm). The expected change in the peak position by a Lorentz correction is greater when the peak is closer to the zero scattering angle. This is the case for SBS and the wax; however, even in this case, the shift is small (less than 10%). The transmission electron micrograph

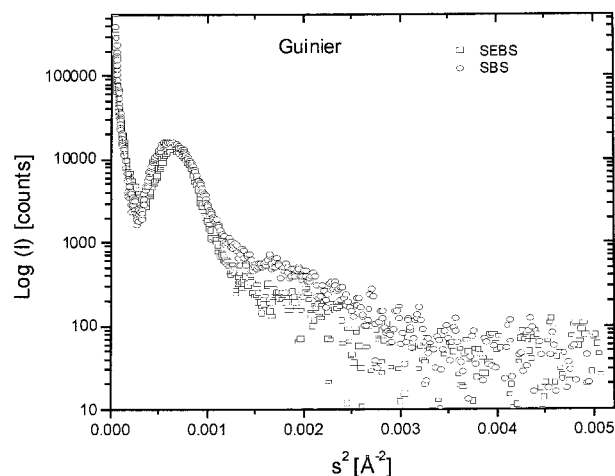


**Figure 11** Desmeared SAXS intensities of styrene/butadiene block copolymers in Guinier representation.

pattern of the blends containing the block copolymer with unsaturation revealed a 25–30-nm periodic arrangement of alternating styrene and butadiene blocks.<sup>21</sup>

## CONCLUSIONS

The experiments performed on different semicrystalline polymers and amorphous block copolymers with narrow molecular weight distributions showed that peaks in the SAXS intensities are present when the system contains periodic structural arrangement. In this case, Lorentz correc-

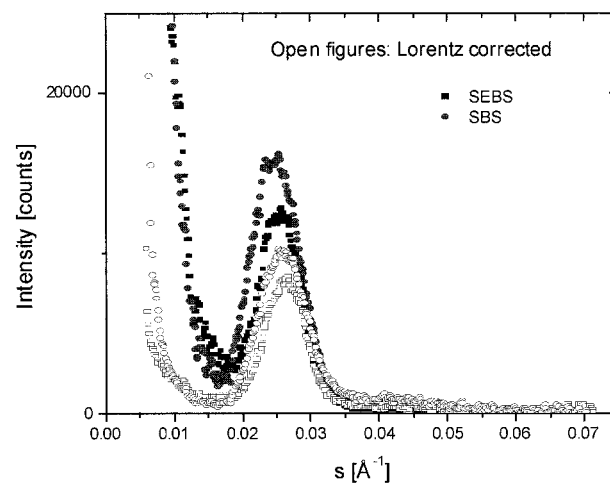


**Figure 12** Desmeared (filled figures) and Lorentz-corrected (open figures) SAXS intensities of styrene/butadiene block copolymers.



tion might result in diffraction peaks corresponding to lesser Bragg periods near to zero diffraction angles.

Many of the semicrystalline polymers like PE did not produce Bragg diffraction peaks at SAXS angles. The reason might be based on structural peculiarities. The source of the scattering is particle type or fractal and there is no Bragg periodicity in the system. Lorentz correction produces artificial Bragg periodicity in these systems. The parameters obtained from the so-called diffraction peaks as result of the applied Lorentz correction are misleading. Lorentz correction, and particularly its squared form, should not be used in the interpretation of SAXS intensities when there is no true indication of the presence of reciprocal lattice scattering. Naturally, the invariant should be calculated in the usual way.

The author is indebted to Dr. J. S. Forsythe (CRC-P) for his contribution in preparing this work.

## REFERENCES

1. Wunderlich, B. *Macromolecular Physics*; Academic Press: New York, 1973.
2. Bassett, D. C. *Principles of Polymer Morphology*; Cambridge University Press: Cambridge, 1981.
3. Capaccio, G.; Ward, I. M.; Wilding, M. A.; Longman, G. W. *Macromol Sci* 1978, B15, 381.
4. Kratky, O. *Pure Appl Chem* 1966, 12, 483.
5. Glatter, O.; Kratky, O. *Small Angle X-ray Scattering*; Academic Press: London, 1982.
6. Guinier, A. *Ann Phys* 1939, 12, 161.
7. Schultz, J. M.; Lin, J. S.; Hendricks, R. W. *J Appl Crystallogr* 1978, 11, 551.
8. Ryan, A. J.; Brass, W.; Mant, G. R.; Derbyshire, G. E. *Polymer* 1994, 35, 4537.
9. Jonas, A. M.; Russel, T. P.; Yoon, D. Y. *Macromolecules* 1995, 28, 8491.
10. Jackson, C. L.; Bauer, B. J.; Nakatami, A. I.; Barnes, J. D. *Chem Mater* 1996, 8, 727.
11. Kavesh, S.; Schultz, J. M. *J Polym Sci Part A* 1970, 8, 243.
12. Dlugosz, J.; Fraser, G. V.; Grubb, D.; Keller, A.; Odell, J. A.; Goggin, L. *Polymer* 1976, B17, 471.
13. Zhou, H.; Wilkes, G. L. *Polymer* 1997, 38, 5735.
14. Peticolas, W. L.; Hibler, G. W.; Lippert, J. L.; Peterlin, A.; Olf, H. *Appl Phys Lett* 1971, 18, 87.
15. Butler, M. F.; Donald, A. M.; Ryan, A. J. *Polymer* 1997, 38, 5521.
16. Russel, T. P.; Koberstein, J. T. *J Polym Sci Polym Phys Ed* 1985, 23, 1109.
17. Narigo, A.; Cingano, G.; Marega, C.; Zannetti, R.; Ferrara, G.; Paganetto, G. *Macromol Chem Phys* 1995, 196, 2537.
18. Koberstein, J. T.; Russel, T. P. *Macromolecules* 1986, 19, 714.
19. Blundell, D. J. *Polymer* 1978, 19, 1258.
20. Schultz, J. M. *J Polym Sci Polym Phys Ed* 1976, 14, 2291.
21. Cser, F.; Rasoul, F.; Kosior, E. *J Polym Eng Sci* 1999, 39, 1100.